Physics of the Solid State, 2022, Vol. 64, No. 5

10,13

Effect of surface and interfaces on longitudinal thermal transport in thin-film Si/Ge structures

© *A.L. Khamets* [1], *I.I. Khaliava* [1], *I.V. Safronov* [2], *A.B. Filonov* [1], *D.B. Migas* [1,3]

[1] Belarusian State University of Informatics and Radioelectronics,
Minsk, Belarus
[2] Belarusian State University,
Minsk, Belarus
[3] National Research Nuclear University „MEPhI",
Moscow, Russia

E-mail: migas@bsuir.by

Received December 17, 2021
Revised December 24, 2021
Accepted December 25, 2021

One of the main approaches to increase the thermoelectric figure of merit of materials is to reduce their thermal conductivity and, in this respect, the surface and possible interfaces play an important role in low-dimensional structures. By means of nonequilibrium molecular dynamics simulations at 300 K we investigate the longitudinal phonon thermal conductivity in Si/Ge multilayered thin-film structures having sharp interfaces and (100), (110), (111) crystallographic orientations with respect to the number of Si/Ge periods (or film thickness) and in comparison with Ge films of equivalent thickness. It is shown that as the thickness of the Si/Ge layered film decreases from ~ 50 to 1 nm and heat flux propagates along the [110] direction, significant phonon-surface scattering occurs for the (100) orientation, which leads to a decrease in the phonon thermal conductivity by almost a factor of 4 (from 19.1 to $5.12\,\mathrm{W/(m\cdot K)}$) and to insignificant change ($\sim 22 \pm 1\,\mathrm{W/(m\cdot K)}$) for the (110) and (111) orientations. In comparison with the Si/Ge films, the Ge films of equivalent thickness display a qualitative and quantitative agreement indicating the scattering of phonons at the Si/Ge interface to be balanced by the higher thermal conductivity of the Si layers.

Keywords: phonon thermal conductivity, thin-films, layered structures, silicon and germanium, molecular dynamics.

DOI: 10.21883/PSS.2022.05.54013.257

1. Introduction

In recent decade, extensive search for new materials for thermoelectric applications has been underway. An essential disadvantage of thermoelectric materials is their low efficiency and hence low efficiency of devices developed on their basis. Efficiency of thermoelectric materials is expressed as dimensionless coefficient ZT which is written as $S^2\sigma T/(\kappa_L + \kappa_e)$, where S, σ, T and κ_L, κ_e are, respectively, the thermoelectric (Seebeck) coefficient, electrical conductivity coefficient, operating temperature and thermal conductivity coefficients (phonon/lattice and electronic components). Currently, one of the most efficient thermoelectric materials include Te-, Bi- and Sb-based compounds whose ZT for p- and n-type materials vary in the range from ~ 1 to 2.5 [1–6]. And for SnSe, one of the highest ZT values equal to ~ 2.6 at 923 K has been found [7].

Currently, a special focus is given to Si and Si-based compounds due to a variety of advantages: proven silicon technology that enables to produce structures with high cost-effectiveness, low toxicity as compared with traditional thermoelectric materials and wide operating temperature range of thermoelectric devices. However, due to its very high thermal conductivity coefficient equal to $140\,\mathrm{W/(m\cdot K)}$ at 300 K, Si has a rather low $ZT \sim 0.01$ at 300 K [8]. As opposed to Si, Ge has a considerably lower thermal conductivity coefficient ($\sim 55\,\mathrm{W/(m\cdot K)}$) [9,10]. It has been defined that the thermoelectric factor ZT for Si-based compounds, SiGe alloys and heavily doped Si materials is within the range from ~ 0.3 to 1.5 [11–16]. For Si and Ge compounds, n-type SiGe alloy shows the highest $ZT = 1.84$ [17]. To achieve the efficiency from 20% to 30% and to put the devices based on thermoelectric materials into wide use, ZT should be equal to $3-4$ [18].

One of the key approaches to increase ZT is to reduce the phonon-based thermal conductivity of the material. For this, low-size semiconductor structures are used, including thin films or nanowires [19]. For example, thermal conductivity in Si thin films depends very much on their thickness and may be reduced as a result of intensive phonon-surface scattering to the values below $10\,\mathrm{W/(m\cdot K)}$ for longitudinal heat transport [20], and in case of high defect content, thermal conductivity can be equal to $4.7\,\mathrm{W/(m\cdot K)}$ with ZT of such structure equal to 0.2 at 360 K [21]. Experiments have also shown significant reduction of thermal conductivity in Si- and Ge-based superlattices as compared with their parent bulk materials due to additional phonon-interface scattering at Si/Ge interfaces [22–25]. In particular,

thermal conductivity in Si/Ge superlattices may be reduced to $\sim 3\,W/(m\cdot K)$ at 300 K [23] depending on the layer thicknesses. The main theoretical research efforts for the same objects have been focused on the investigations of thermal conductivity depending on the period length in symmetric periodic superlattices [26–33] and asymmetrical aperiodic superlattices [34], on interface structure (including roughness and/or interdiffusion [26,27,29,30,33]), and temperature [29,30,33]. However, there are hardly any papers where thermal conductivity in thin superlattices, i.e. layered films with few periods, is addressed. Transverse thermal conductivity assessed by non-equilibrium molecular dynamics method in Si/Ge symmetrical layered films [35] and for the Boltzmann transport equation for Si/Ge superlattices [36] were reported. It is not excluded that an additional thermal conductivity reduction factor may include selection of superlattice surface orientation. The influence of this effect on thermal conductivity was discussed before only for homogenous Si thin films [37–39] for which the highest phonon-surface scattering efficiency was determined for Si(100) surface. It should be noted that theoretical study has only covered Ge(100) thin films where significant anisotropy was found for longitudinal and transverse thermal conductivity components depending on thickness [40] and significant influence of surface roughness on thermal conductivity [41]. No longitudinal thermal conductivity of Si/Ge layered films and Ge thin films depending on the surface orientation and number of periods or thickness is reported. Thus, the purpose of the research is to investigate the influence of the surface and interface in Si/Ge multilayer thin-film structures on longitudinal phonon thermal conductivity as compared with homogenous Ge films for (100), (110) and (111) orientations.

2. Materials and research techniques

The scope of study included (100)-, (110)- and (111)-oriented layered thin film structures in the form of symmetrical Si/Ge heterostructures with sharp interfaces and homogenous Si and Ge films with equivalent thickness. The number of periods varied with constant thickness of Si and Ge layers that was assumed equal to 4 monoatomic layers for (100) and (110) orientations and 6 monoatomic layers for (111) orientation to avoid morphologies with islands on Ge surface[42]. The period herein means Si/Ge bilayer. $p(2\times 1)$, $p(1\times 1)$ and $p(2\times 1)$ surface reconstructions were used, respectively, for both homogenous and layered films with (100), (110) and (111) orientations. For preparation and visualization of all structures, Jmol [43] and OVITO were used [44]. Data acquired for Si/Ge bulk array without surface and with various Si/Ge interface orientations was also used for comparison.

Structural optimization of Si/Ge layered thin film structures was performed using the molecular statics method implemented in LAMMPS software package [45]. Total system energy was minimized taking into account the relaxation and optimization of the atomic structure geometry with variable super cell. Three-dimensional periodic interface conditions with a vacuum gap of ~ 2 nm above the layer stacking plane were used to simulate a thin film structure. Interatomic interaction for the Si−Ge system was described using the Tersoff potential [46]. This potential can reliably predict thermodynamic properties of bulk Si [47], Ge [47], Si−Ge solid solutions [46], and has been used before for thermal conductivity simulation of Si/Ge films [32,35,48,49].

The phonon component of thermal conductivity was simulated by the non-equilibrium molecular dynamics method implemented in LAMMPS [45]. The time interval was taken equal to 1 fs. At the first simulation stage, the structures were brought to thermodynamic equilibrium by means of isobaric-isothermal and canonical ensembles during 0.1 ns each at $T = 300$ K. A microcanonical ensemble was used during 1 ns at the second simulation stage to establish thermodynamic equilibrium. The layer temperature was monitored and maintained using Langevin thermostats with input of the corresponding damping coefficients which affect the relaxation time during oscillations due to the different atomic masses. Two thermostats were used to provide a temperature gradient in the structures: a cold ($T = 290$ K) and a hot one ($T = 310$ K) at the distance equal to the supercell half-size in the heat flow direction. It should be noted that when using the non-equilibrium molecular dynamics method, the calculated thermal conductivity coefficient depends on the size of the supercell along which the heat flows, when the supercell size is smaller than or comparable to the mean free path of phonons at the given temperature. The frequent underestimation (understatement) of thermal conductivity values is avoided by increasing the supercell size which requires too much computational effort, but has no any significant impact on the thermal conductivity trends. It is believed that to use the Fourier law, linear response conditions between inverse thermal conductivity and supercell length shall be achieved. According to the authors of [47], for example, the inverse thermal conductivity for Si crystal becomes linearly dependent on the inverse supercell length, when the latter achieves the sizes > 100 nm. Taking into account the fact that the mean phonon free path (thermal conductivity vs. heat capacity and average phonon velocity) in Ge crystal will be lower than for Si (~ 300 nm [50]), the linear response conditions shall be also fulfilled in this case with the chosen supercell size. Based on these conclusions, all Si/Ge multilayer thin film structures addressed herein had a supercell size of ~ 100 nm in the heat flow direction along the layers. The Si/Ge structure cross-section was assumed as $\sim 60\,nm^2$.

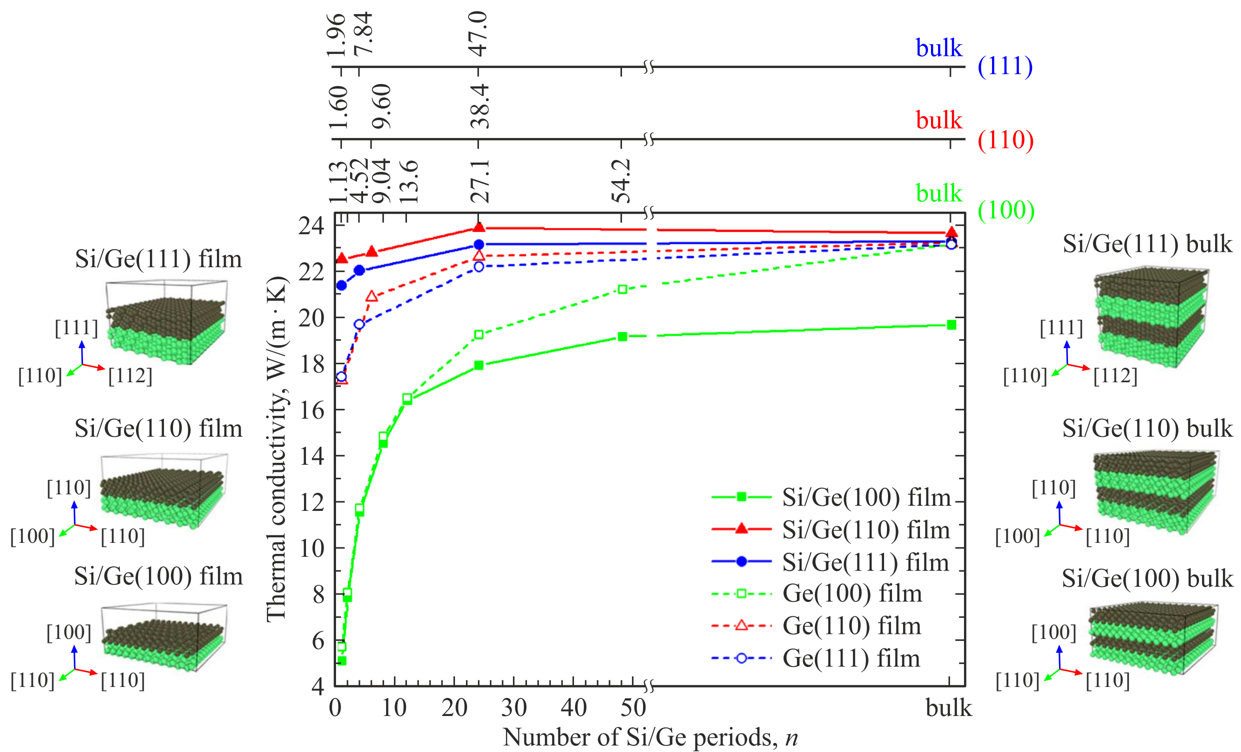

Longitudinal phonon thermal conductivity in [110] direction at 300 K and models of Si/Ge layered thin film structures with (100), (110) and (111) orientations depending on the number of periods. Applicable thicknesses for Ge films are shown on three upper axes in nm.

The phonon thermal conductivity coefficient (κ_L) was defined according to the Fourier law:

$$\kappa_L = -\frac{E}{2S_{sec} \cdot t \cdot (dT/dx)},$$

where E is the transferred thermal energy; 2 is the coefficient related to heat flow in two directions; t is the simulation time; S_{sec} is the cross-section area; dT/dz is the temperature gradient in [110] direction. The phonon thermal conductivity coefficient was calculated after 2 ns of simulation.

3. Results and discussion

Due to the cubic symmetry of Si and Ge crystals, [110] direction exists for films of these materials with (100), (110) and (111) orientations which allows to compare the contribution of the Si/Ge surface and interface to phonon scattering in heat flow along this direction for all investigated nanostructures. The Figure shows the dependence of the longitudinal thermal conductivity (in [110] direction) on the number of periods in Si/Ge multilayer thin film structures and in homogeneous Ge films with the equivalent thickness and (100), (110) and (111) surfaces. The presence of orientation effect, which means different longitudinal thermal conductivity saturation rate in the considered structures, is evident. For Si/Ge layered films, when the number of periods is increased from 1 to 48, significant increase (almost by a factor of 4) in the longitudinal phonon thermal conductivity is observed for (100) oriented Si/Ge structures from 5.12 to 19.1 W/(m · K), while for Si/Ge(110) and Si/Ge(111) structures, only a small increase was observed from 22.5 to 23.6 W/(m · K) and from 21.4 to 23.3 W/(m · K), respectively. Increase in the longitudinal thermal conductivity with the increase in the number of periods may be explained by the layer-restricted and extended heat transfer concept [30] which shows that the increase in the number of periods has higher contribution to the phonon thermal conductivity because more and more phonons can intersect the interfaces and propagate in the overlying layers (see the Figure). On the other hand, the role of the phonon scattering over surface is also obvious, since only Si/Ge(100) structures are characterized by significant decrease in thermal conductivity with the decrease in the number of periods (and number of Si/Ge interfaces and film thickness).

Similar dependences also occur for Ge films (see the Figure). With the increase in their thickness (from ~ 1 nm to the bulk), increase in the thermal conductivity is observed: from 5.72 to 23.1 W/(m · K), from 17.3 to 23.1 W/(m · K) and from 17.4 to 23.1 W/(m · K), respectively, for (100), (110) and (111) orientations. Like for Si/Ge(100) layered films, significant (x4) increase in thermal conductivity is observed for homogeneous Ge(100) films with the increase in thickness which is not the case for (110) and (111) orientations.

A similar trend has been observed before for Si thin films when their thickness was changed (10 nm and lower) as a result of redistribution of phonon-phonon and phonon-surface scattering as well as phonon depletion effect [51]. In case of longitudinal heat transport in Si thin films in [110] direction, not only the phonon scattering rates (inverse to the relaxation time), but also group phonon velocities (proportional to thermal conductivity) are different [38,39]. The authors of [39] have shown that the average-weighted frequency dependence curve for all group phonon velocity modes for Si(110) lies higher than that for Si(100) and Si(111). For phonon scattering, the analysis of the phonon constant energy surface shapes for Si crystal in [38] has shown that (100) surfaces have the maximum scattering capability for longitudinal heat transport in Si thin films. For the addressed Si/Ge layered structures and homogeneous Ge films, their longitudinal thermal conductivity is defined both by the group phonon velocity and phonon scattering relaxation time that are the highest for (110) orientation and the lowest for (100) orientation which explain and result in the dependence shown in the Figure.

Taking into account that the thermal conductivity of bulk Ge ($\sim 55\,\mathrm{W/(m \cdot K)}$ [9,10]) is ~ 2.5 times lower that for Si ($\sim 140\,\mathrm{W/(m \cdot K)}$ [52,53]), potential advantage in terms of the decrease in the thermal conductivity of Si/Ge layered thin film structures compared with homogeneous Ge films is due to the Si/Ge interfaces. Such advantage exists for (100) orientation, while for (110) and (111) orientations, the opposite trend is observed (see the Figure). This means that the phonon-interface scattering in the first case compensates for the contribution to the total thermal conductivity of more thermally-conductive Si layers. However, only for (100) orientation, the difference in the thermal conductivity for Si/Ge layered thin film structure and homogeneous Ge film with the equivalent thickness is increased from ~ 10.5 to 17.3% when the number of periods is increased from one to bulk, respectively. This is due to the fact that for the Si/Ge(100) layered film, the increase in the number of interfaces results in more intense phonon scattering compared with the homogeneous Ge film, while for Si/Ge(110) and Si/Ge(111), phonon scattering at the interfaces is lower and the differences are only apparent with a small number of periods when free surfaces have an additional influence.

As compared with homogeneous Si films with the equivalent thickness, the Si/Ge layered films have a lower thermal conductivity. With the increase in the Si(100) film thickness from 1.09 to 52.8 nm (equivalent Si/Ge structure thickness increased from 1 to 48 periods, respectively), thermal conductivity is increased from 10.9 to $34.3\,\mathrm{W/(m \cdot K)}$, which is by $\sim 45-50\%$ higher than that of the Si/Ge thin film structure with the equivalent thickness. For Si(110) and Si(111) orientations, a similar trend is observed and phonon thermal conductivities for thin films with these orientations are by $\sim 45\%$ higher than in Si/Ge layered thin film structures with the equivalent thickness (not shown in the Figure).

For the Si/Ge bulk superlattice, the difference in thermal conductivities depending on the interface orientations is clearly visible, in particular for Si/Ge(100). I.e., despite the absence of surfaces, the thermal conductivity values do not converge as opposed to bulk Ge (see the Figure). This demonstrates an essential role of the Si/Ge interfaces with such plane orientation that provides the most intense phonon scattering. The latter is attributed to the fact that phonon movement directions do not coincide with the prevailing phonon scattering directions during the longitudinal heat transfer. Therefore, as shown in the Figure, the Si/Ge bulk superlattices with (110) and (111) interface orientations have no priority over Ge single crystals.

Additional calculations have been carried out for Si/Ge layered thin film structures with added Si or Ge surface layers in order to obtain both terminating heterostructure surfaces from the same material. For (100) orientation, almost no considerable changes in the thermal conductivity dependence on the number of periods (thickness), as shown in the Figure, were observed both for Si and Ge surface layers. For (110) and (111) orientations, decrease (or increase) in thermal conductivity was observed at $3-4\,\mathrm{W/(m \cdot K)}$ with $\sim 10\,\mathrm{nm}$ thicknesses, if both surface layers are formed by Ge (or Si) atoms. However, this effect is very quickly neutralized at thicknesses within $\sim 32-39\,\mathrm{nm}$ (not shown in the Figure). Thus, for Si/Ge(110) and Si/Ge(111) thin film structures, their thermal conductivity may be additionally changed by selecting the terminating surface material, but only at film thicknesses lower than $\sim 10\,\mathrm{nm}$.

4. Conclusion

Calculations of the longitudinal phonon thermal conductivity in homogeneous Ge films and Si/Ge layered thin film structures with (100), (110) and (111) orientations depending on their thickness carried out using the non-equilibrium molecular dynamics method have shown similar dependences. Compared with (110) and (111) orientations, films with (100) orientations are characterized by the lowest thermal conductivities and significant thermal conductivity changes depending on thickness which demonstrates the presence of orientational effect in case of heat flow in [110] direction. This effect is mainly attributed to the surface while, for Si/Ge films, the interfaces scatter phonons to a lesser extent. It should be noted that for Si/Ge and Ge films with the equivalent thickness, quantitative data is comparable. This means that, compared with Ge films, phonon-interface scattering in Si/Ge films neutralizes, or does not neutralize, the contribution of more thermally-conductive Si layers. Only for Si/Ge(100) films, decrease in thermal conductivity by $\sim 10.5-17.3\%$ was observed compared with homogeneous Ge(100) films with the increase in the number of periods, i.e. in the range of hundreds nm significant decrease in thermal conductivity is possible due to additional scattering at the interfaces. The

findings demonstrate that the phonon thermal conductivity of Si/Ge layered thin film structures may be changed by changing the number of Si/Ge periods and selecting the appropriate crystal-lattice orientation. However, for more accurate efficiency assessment of thermoelectric devices based on the given nanostructures, possible change in the power factor and temperature influence on thermal conductivity shall be additionally investigated as well as longitudinal thermal conductivity and thermal conductivity in other crystal-lattice directions shall be further investigated.

Acknowledgments

The authors express their gratitude to professor N.A. Poklonsky (Belorussian State University) for fruitful discussions.

Funding

The research has been performed under the state scientific program of the Republic of Belarus „Material science, new materials and technologies“.

Conflict of interest

The authors declare that they have no conflict of interest.

References

[1] J.P. Heremans, V. Jovovic, E.S. Toberer, A. Saramat, K. Kurosaki, A. Charoenphakdee, S. Yamanaka. Science **321**, *5888*, 554 (2008).
[2] L. Hu, T. Zhu, X. Liu, X. Zhao. Adv. Func. Mater. **24**, *33*, 5211 (2014).
[3] Y. Pei, A. LaLonde, S. Iwanaga, G. Jeffrey Snyder. Energy Environ. Sci. **4**, *6*, 2085 (2011).
[4] A.D. LaLonde, Y. Pei, G. Jeffrey Snyder. Energy Environ. Sci. **4**, *6*, 2090 (2011).
[5] Pierre F.P. Poudeu Dr., J. D'Angelo, A.D. Downey, J.L. Short, T.P. Hogan, M.G. Kanatzidis. Angewandte Chem. Int. Ed. **45**, *23*, 3835 (2006).
[6] G. Tan, F. Shi, S. Hao, Li-Dong Zhao, H. Chi, X. Zhang, C. Uher, C. Wolverton, Vinayak P. Dravid Mercouri G. Kanatzidis. Nature Commun. **7**, 12167 (2016).
[7] Li-Dong Zhao, Shih-Han Lo, Y. Zhang, H. Sun, G. Tan, C. Uher, C. Wolverton, V.P. Dravid, M.G. Kanatzidis. Nature **508**, 373 (2014).
[8] T.H. Geballe, G.W. Hill. Phys. Rev. **98**, *4*, 940 (1955).
[9] A.F. Ioffe. Can. J. Phys. **34** (12A), 1342 (1956).
[10] V.I. Ozhogin, A.V. Inyushkin, A.N. Taldenkov, A.V. Tikhomirov, G.É. Popov, E. Haller, K. Itoh. J. Exp. Theor. Phys. Lett. **63**, 490 (1996).
[11] J.P. Dismukes, L. Ekstrom, E.F. Steigmeier, I. Kudman, D.S. Beers. J. Appl. Phys. **35**, *10*, 2899 (1964).
[12] V. Kessler, D. Gautam, T. Hülser, M. Spree, R. Theismann, M. Winterer, H. Wiggers, G. Schierning, R. Schmechel. Adv. Eng. Mater. **15**, *5*, 379 (2012).
[13] C.B. Vining, W. Laskow, J.O. Hanson, R.R. Van der Beck, P.D. Gorsuch. J. Appl. Phys. **69**, *8*, 4333 (1991).
[14] X.W. Wang, H. Lee, Y.C. Lan, G.H. Zhu, G. Joshi, D.Z. Wang, J. Yang, A.J. Muto, M.Y. Tang, J. Klatsky, S. Song, M.S. Dresselhaus, G. Chen, Z.F. Ren. Appl. Phys. Lett. **93**, *19*, 193121 (2008).
[15] S. Bathula, M. Jayasimhadri, N. Singh, A.K. Srivastva, J. Pulikkotil, A. Dhar, R.C. Budhani. Appl. Phys. Lett. **101**, *21*, 213902 (2012).
[16] A. Yusufu, K. Kurosaki, Y. Miyazaki, M. Ishimaru, A. Kosuga, Y. Ohishi, H. Muta, S. Yamanaka. Nanoscale **6**, *22*, 13921 (2014).
[17] R. Basu, S. Bhattacharya, R. Bhatt, M. Roy, S. Ahmad, A. Singh, N. Navaneethan, Y. Hayakawa, D.K. Aswai, S.K. Gupta. J. Mater. Chem. A **2**, *19*, 6922 (2014).
[18] A.F. Ioffe. Poluprovodnikovyie termoelementy. Izd-vo AN SSSR, M, (1956) (in Russian) 103 s.
[19] J.A. Pérez-Taborda, O. Caballero-Calero, M. Martín-González. New Research on Silicon — Structure, Properties, Technology. InTechOpen. London. (2017). P. 183.
[20] C. Jeong, S. Datta, M. Lundstorm. J. Appl. Phys. **111**, *9*, 093708 (2012).
[21] N.S. Bennett, N.M. Wight, S.R. Popuri, Jan-Willem G. Bos. Nano Energy **16**, 350 (2015).
[22] S.-M. Lee, David G. Cahill, R. Venkatasubramanian. Appl. Phys. Lett. **70**, *22*, 2957 (1997)
[23] T. Borca-Tasciuc, W. Liu, J. Liu, T. Zeng, David W. Song, C.D. Moore, G. Chen, Kang L. Wang, M.S. Goorsky, T. Radetic, R. Gronsky, T. Koga, M.S. Dresselhaus. Superlat. Microstruct. **28**, *3*, 199 (2000).
[24] W.L. Liu, T. Borca-Tasciuc, G. Chen, J.L. Liu, K.L. Wang. J. Nanosci. Nanotechnology **1**, *1*, 39 (2001)
[25] S. Chakraborty, C. A. Kleint, A. Heinrich, C.M. Schneider, J. Schumann, M. Falke, S. Teichert. Appl. Phys. Lett. **83**, *20*, 4184 (2003).
[26] E.S. Landry, A.J.H. Mc Gaughey. Phys. Rev. B **79**, *7*, 075316 (2009).
[27] J. Grag, G. Chen. Phys. Rev. B **87**, *14*, 140302 (2013).
[28] Keng-Hua Lin, A. Strachan. Phys. Rev. B **87**, *11*, 115302 (2013).
[29] Z. Aksamija, I. Knezevic. Phys. Rev. B **88**, *15*, 155318 (2013).
[30] K. Kothari, M. Maldovan. Sci. Rep. **7**, 5625 (2017).
[31] H. Dong, B. Wen, Y. Zhang, R. Melnik. RSC Advances **7**, *48*, 29959 (2017).
[32] A. Kandemir, A. Ozden, T. Cagin, C. Sevik. Sci. Technol. Adv. Mater. **18**, *1*, 187 (2017).
[33] G.P. Srivastava, Lorwerth O. Thomas. Nanomaterials **10**, 673 (2020).
[34] J. Yan, H. Wei, H. Xie, X. Gu, H. Bao. ES Energy Environment **8**, 56 (2020)
[35] V. Samvedi, V. Tomar. J. Appl. Phys. **105**, *1*, 013541 (2009).
[36] A. Malhotra, K. Kothari, M. Maldovan. J. Appl. Phys. **125**, *4*, 044304 (2019).
[37] P. Heino. Eur. Phys. J. B **60**, 171 (2007).
[38] Z. Aksamija, I. Knezevic. Phys. Rev. B **82**, *4*, 045319 (2010).
[39] H. Karamitaheri, N. Neophytou, H. Kosina. J. Appl. Phys. **113**, *20*, 204305 (2013).
[40] X. Zhang, X. Wu. Comput. Mater. Sci. **123**, 40 (2016).
[41] Z.H. Wang, M.J. Ni. Heat Mass Transfer **47**, 449 (2011).
[42] B. Voigtländer. Surface Sci. Rep. **43**, *5–8*, 127 (2001).
[43] Jmol: an open-source Java viecer for chemical structures in 3D. http://www.jmol.org/
[44] A. Stukowski. Mod. Simul. Mater. Sci. Eng. **18**, 015012 (2009).

[45] S. Plimpton. J. Comp. Phys. **117**, 1 (1995).
[46] J. Tersoff. Phys. Rev. B **39**, *8*, 5566 (1989).
[47] Y. He, I. Savić, D. Donadio, G. Galli. Phys. Chem. Chem. Phys. **14**, *47*, 16209 (2012).
[48] Z. Wang. Mater. Today Commun. **22**, 100822 (2020).
[49] A. Giri, Jeffrey L. Braun, Patrick E. Hopkins. J. Appl. Phys. **119**, *23*, 235305 (2016).
[50] Y.S. Ju, K.E. Goodson. Appl. Phys. Lett. **74**, *20*, 3005 (1999).
[51] X. Wang, B. Huang. Sci. Rep. **4**, 6399 (2014).
[52] H.R. Shanks, P.D. Maycock, P.H. Sidles, G.C. Danielson. Phys. Rev. **130**, *5*, 1743 (1963).
[53] W.S. Capinski, H.J. Maris. E. Bauser, I. Silier, M. Asen-Palmer, T. Ruf, M. Cardona, E. Gmelin. Appl. Phys. Lett. **71**, *15*, 2109 (1997).